



LAWRENCE
LIVERMORE
NATIONAL
LABORATORY

Simulation of triple ion-beam irradiation in Fe single crystals using stochastic cluster dynamics

J. Marian, T. Hoang

July 14, 2014

Disclaimer

This document was prepared as an account of work sponsored by an agency of the United States government. Neither the United States government nor Lawrence Livermore National Security, LLC, nor any of their employees makes any warranty, expressed or implied, or assumes any legal liability or responsibility for the accuracy, completeness, or usefulness of any information, apparatus, product, or process disclosed, or represents that its use would not infringe privately owned rights. Reference herein to any specific commercial product, process, or service by trade name, trademark, manufacturer, or otherwise does not necessarily constitute or imply its endorsement, recommendation, or favoring by the United States government or Lawrence Livermore National Security, LLC. The views and opinions of authors expressed herein do not necessarily state or reflect those of the United States government or Lawrence Livermore National Security, LLC, and shall not be used for advertising or product endorsement purposes.

This work performed under the auspices of the U.S. Department of Energy by Lawrence Livermore National Laboratory under Contract DE-AC52-07NA27344.

Simulation of triple ion-beam irradiation in Fe single crystals using stochastic cluster dynamics

Jaime Marian, Tuan Hoang
Lawrence Livermore National Laboratory

Abstract

Helium and hydrogen are produced at rates of about 10 and 40 appm per dpa during fusion reactor operation. Although, the effects of He and H on microstructure are more or less well understood independently, their combined action under irradiation has not been established yet and the experimental evidence obtained over three decades of research is inconclusive. In recent years, electronic structure calculations have shed some light on the joint effect of He and H on defect cluster stability, and the associated energetics has begun to be used in long-term models of damage accumulation. In this work, we present stochastic cluster dynamics (SCD) simulations of triple (Fe/He/H) ion beam irradiations of pure single crystal Fe. With SCD we can perform simulations of multiple damage species up to doses beyond the 1-dpa limit. We calculate the amount of swelling as a function of temperature and point to the limitations of the He/H interaction model by comparing and discussing the experimental data.

1 Introduction: Fusion structural materials

One scientific challenge for fusion energy is to develop an understanding of the response to radiation damage accumulation of the first wall and breeding-blanket materials that will likely determine the operating parameters and hence the energy efficiency (operating temperature) and overall lifetime of any fusion reactor. The structural materials of a fusion reactor are exposed to a hard neutron spectrum that results in atomic displacement cascades and transmutation nuclear reactions. The displacement cascades produce vacancies, interstitials, and a variety of extended defects, but of particular concern is the simultaneous production of helium and hydrogen at dose rates and accumulated concentrations for which the materials and engineering communities have little practical experience and hence little understanding.

2 Displacement damage and the generation of He and H

The rate of atomic displacements per atom (dpa) will amount to 20-30 dpa/year in steels, while the He and H gas produced by transmutation nuclear reactions will be 10-15 appm and 40-50 appm per dpa respectively, all of which are produced continuously and simultaneously. There is considerable experience both experimental and modeling for low dpa production simultaneously with He that is relevant to fission reactors [1]. In fusion conditions, the dpa and He rates are one to two orders of magnitude greater, and whose effects are the object of careful experimental characterization [2], but the simultaneous transmutation production of H introduces a new variable for which little experimental data and modeling exist.

2.1 Transmutation production of gas atoms

Nuclear reactions (n, α), (n,p), and (2n,p) from neutrons result in the transmutation production of the gas atoms He and H. In a comparison of a fission reactor neutron spectrum and a computed DEMO neutron spectrum it is observed that the fluxes per lethargy unit are greater for the fusion spectrum at all energies above 2 MeV [3]. It is noted in [4] that because of inadequacy of the modeling of the DEMO spectrum, the fusion flux below 2 MeV may also be greater than the fission spectrum. Moreover because every fusion reaction yields a 14.1 MeV neutron there is a peak in the neutron spectrum at that energy.

The production and retention of H in combination with He in fission reactor fcc austenitic steels has been established experimentally [5], along with some early evidence for the synergistic consequences of simultaneous H and He production together with displacement damage. While this discovery identified interesting degradation of the irradiated steels associated with the synergy of H and He, in fusion the consequences of transmutation gas production are unknown, although it would not be unreasonable to expect them to result in more serious problems because of the much higher production rates and the much greater desired lifetime doses.

3 Experimental evidence for He-H synergies:

In a 1994 report to General Atomics, Bullough reviewed the current understanding of possible radiation effects in vanadium alloy and in the ferritic-martensitic (F/M) steel 9Cr-1Mo known as T91 (also P91). It is noted that dual ion-beam data on pure vanadium shows evidence for both helium and hydrogen leading to significant swelling in pure vanadium in the presence of simultaneous production of atomic displacement damage from heavy ion irradiation [6]. It is emphasized in this report that an important issue for F/M steel application as the fusion first wall material was (and still is today) “Resistance to irradiation damage in the presence of the helium and hydrogen that will be produced by the high-energy fusion neutrons.....” [6]. While the development of core materials for fast fission reactors benefited from the availability of testing reactors, no such facilities exist today for the development of fusion materials. This then leaves us with a strategy of accumulating data from simulation experiments that inform and are understood through coupling to computational models. Unfortunately, this approach is not without uncertainty arising from unexpected phenomena or from the difference between the simulation conditions and those of an actual fusion facility; dose rate, details of the damage cascade arising from the kinetics of the cascade inducing particle, specimen dimensions, and details of the chemistry, phase and microstructural features of the material under test. Early evidence for a He and H synergy in the presence of displacement damage in F/M steel (1986) was given by Farrell and Lee [7] who investigated the combined effects of the high input of He and H along with displacement damage using multiple simultaneous ion beams (MSIB) of He, H, and Fe and reported a rather significant increase in the peak swelling rate in 12Cr-1Mo steel.

It is useful to note that while the primary motive for understanding the synergistic role of displacement damage and He and H production in F/M steels comes from a need to identify radiation tolerant materials for fusion energy this same challenge became a

research issue for fission energy austenitic steels when it was suggested that hydrogen might serve the same role as helium in stabilizing small vacancy clusters to form bubbles that once reaching critical size lead to void formation [8]. Because hydrogen is a fast diffuser it was commonly held that hydrogen in austenitic (stainless steels) steels could not be retained at high concentrations and would diffuse out. Experimental work led to the discovery that hydrogen, which is produced by nuclear reactions but which is also introduced into steels by a variety of other processes both nuclear and chemical, is retained when helium nucleated cavities become a significant part of the microstructure [9].

4 Modeling triple Fe/He/H implantation:

4.1 Experimental and computational evidence of vacancy/He/H interactions in Fe

Results obtained from positron annihilation lifetime and coincidence Doppler broadening measurements indicate that He atoms are more effective for micro-void formation than H atoms [10]. Therefore, He will first form bubbles with existing vacancy clusters. As He bubbles grow due to absorption of more He and vacancies in the volume, their surface areas increase and the surrounding stress fields attract H atoms towards them [11] and form the V-He-H triple clusters. This would also explain the existence of an incubation time for V-He-H clusters to form, and the higher the He⁺ damage rate is, the sooner these triple clusters appear. The presence of He within the crystal has been proved experimentally to significantly enhance the trapping of hydrogen, even for periods of years after irradiation [12-14]. Comparing the vacancy cluster number densities in the specimens for the two cases of dual (Fe³⁺+He⁺) ion-irradiation and triple ion-irradiation, we see that the presence of hydrogen under triple ion-irradiation condition has caused a reduction in vacancy cluster and vacancy-He bubble populations.

For its part, the computational characterization of V/He/H interaction effects come from three main sources. Kirsanov et al. [15] noted that the small binding energy of H and its high mobility in bulk Fe allows them to find otherwise mobile He-2V clusters and attach itself to the free vacancy. He-2V clusters are the main carriers of He during gas void formation, and thus one may expect a delay of helium bubble formation caused by H, and an increased number of nucleation sites. Using DFT calculations, Hayward and Deo [16] analyzed the energetics and structure of small V-He-H bubbles, and explained the seemingly observed He/H synergy as a consequence of bubble growth through helium induced loop punching, aided by the presence of H, instead of as a direct interaction between H and He. The H benefits from an increased area of free surface on which to bind. However, we discount this possibility, as it would require insertion doses much in excess of those present in fusion environments. Finally, Ortiz et al. [17] also performed DFT calculations of V-He-H complexes and obtained a weak interaction between H and He in bubbles. This is in contrast to previous DFT results of a strong trapping of H at He. The strong preference of He and H to occupy regions with low electronic density (such as vacancies) explains this discrepancy, with vacancy-He and vacancy-H binding forces screening the repulsive interaction between He and H.

4.2 Model of bubble formation in Fe in the presence He and H atoms

Based on the evidence put forward in the preceding section, we implement the following model of V/He/H interaction:

- Both He and H atoms display extremely fast three-dimensional diffusion and cover the entire configurational space very efficiently.
- Small vacancy clusters can attract H atoms. However, these atoms do not occupy substitutional vacant sites. Instead they bind (with binding energy: 0.5 eV) at external tetra or octahedral interstitial positions. Thus, they do not intrinsically stabilize small vacancy clusters.
- He atoms can stabilize small vacancy clusters by occupying vacant sites. However, these V-He complexes can retain some mobility particularly if the number of He atoms is not equal to the number of vacancies.
- If a H finds one of these mobile V-He complexes, turning it into a V-He-H complex, their mobility is then suppressed.
- It is assumed that triple V-He-H clusters are stable across the entire temperature range, such that no vacancies, helium or hydrogen can detrapp from these clusters.

The implicit temperature dependence of the above model stems from the competition between two main mechanisms. At lower temperatures, H and He atoms are more strongly bound to V-H and V-He clusters respectively (more potential nucleation points), but the mobility of these clusters is small and there is less coalescence as well as losses to sinks. At high temperatures, nucleated bubbles can coalesce giving rise to larger bubbles, but losses to sinks increase. The optimum compromise is found and the so-called peak swelling temperature.

As well, when we increase the He damage rate, the population of V-He-H clusters also increases. However swelling may decrease because, as more helium is inserted into the volume, the number of nucleated V-He bubbles also increases, but they become smaller because helium atoms will now combine with many smaller vacancy clusters instead of few larger ones. Because of that, the stress fields around these V-He bubbles are weaker, and the amount of hydrogen atoms attracted to them decreases accordingly. As V-He clusters become smaller, the reactions between hydrogen and these clusters are less likely to take place. This leads to the decrease of the stable V-He-H cluster population which is the main cause of volume swelling in materials under multi-ion irradiation. On the other hand, loading more hydrogen into the volume causes more swelling due to the increase of the stable V-He-H triple cluster population. Thus, we can see that the He:H ratio directly effects the amount of volume swelling and the formation of defect clusters in the materials.

4.3 Stochastic cluster dynamics method for long-term damage accumulation

Here we use the stochastic cluster dynamics method (SCD) [18] to perform all simulations. SCD is a stochastic variant of the mean-field rate theory technique, alternative to the standard ODE-based implementations, that eliminates the need to solve exceedingly large sets of ODEs and relies instead on sparse stochastic sampling from the underlying kinetic master equation. Rather than dealing with continuously varying defect

concentrations in an infinite volume, SCD evolves an integer-valued defect population N_i in a finite material volume V , thus avoiding combinatorial explosion in the number of ODEs. This makes SCD ideal to treat problems where the dimensionality of the cluster size space is high, e.g., when multispecies simulations—for example involving energetic particles, He, H, etc., simultaneously—are of interest. SCD recasts the standard ODE system into stochastic equations of the form:

$$\frac{dN_i}{dt} = \tilde{g}_i - \sum_j \tilde{s}_{ij} N_i + \sum_j \tilde{s}_{ji} N_j - \sum_{i,j} \tilde{k}_{ij} N_i N_j + \sum_{j,k} \tilde{k}_{jk} N_j N_k$$

where the set $\{\tilde{g}, \tilde{s}, \tilde{k}\}$ represents the reaction rates of 0th (insertion), 1st (thermal dissociation, annihilation at sinks), and 2nd (binary reactions) order kinetic processes taking place inside V . Calculations involving clusters with three dimensions in the number of species are costly in computation and memory, and have been brought about by the implementation of several enhancements to SCD, such as τ -leaping and volume re-scaling [19].

For the SCD calculations, the baseline parameterization is that used by Marian and Bulatov [18], to which the damage/He/H model described in Section 4.2 is added in terms of additional energetics and specification of extra key reactions. By way of example, we show in Figure 1 the PKA cumulative damage function that defines the source term.

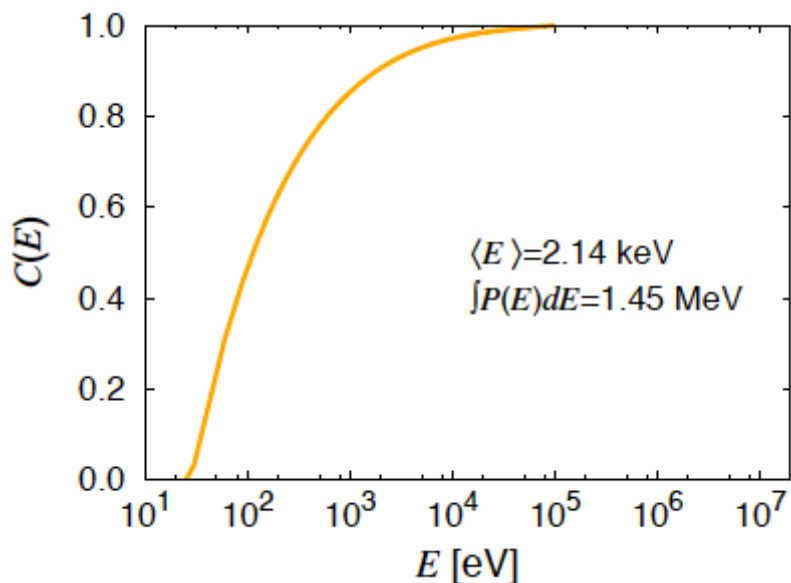


Figure 1: Cumulative damage function for 10.5-MeV Fe ions in Fe from SRIM calculations. The average PKA energy from this function is $\langle E \rangle = 2.14$ keV, while the total damage energy is 1.45 MeV.

$C(E)$ is sampled during every insertion event and defect distributions are generated from existing cascade statistics for every PKA energy E . This process is repeated until the total damage energy of 1.45 MeV is reached. This process completes a full insertion event, which occurs at a rate consistent with the prescribed dose rate.

5 Calculations

The calculations are run up to a total dose of 1 dpa and all defect populations are tallied as a function of dose. Figure 2 shows the evolution of the defect species with dose at a temperature of 510°C. The calculations reveal interesting information, such as the incubation times of each species subpopulation, or the metastability of certain types of clusters.

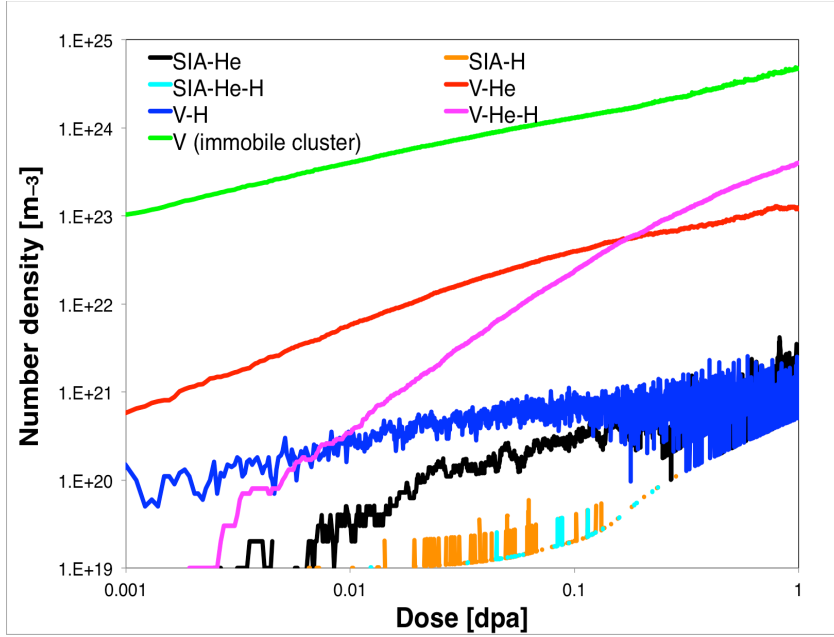


Figure 2: Evolution with dose of all defect species at a temperature of 783 K.

The total amount of swelling can be calculated by summing over the number of vacancies contained in all stable, immobile vacancy clusters, and dividing by the number of lattice sites in the simulation volume:

$$S = \frac{\Omega_a \sum_i^{N_V} n_i}{\Omega \rho_a}$$

This swelling ratio is plotted in Figure 3 as a function of dose at the four temperatures considered in this study. As the figure shows, the differences are not remarkable, although a clear temperature dependence can be distinguished. This is what is shown in the inset, where a peak swelling temperature of around 800 K can be appreciated for the swelling levels after 1 dpa.

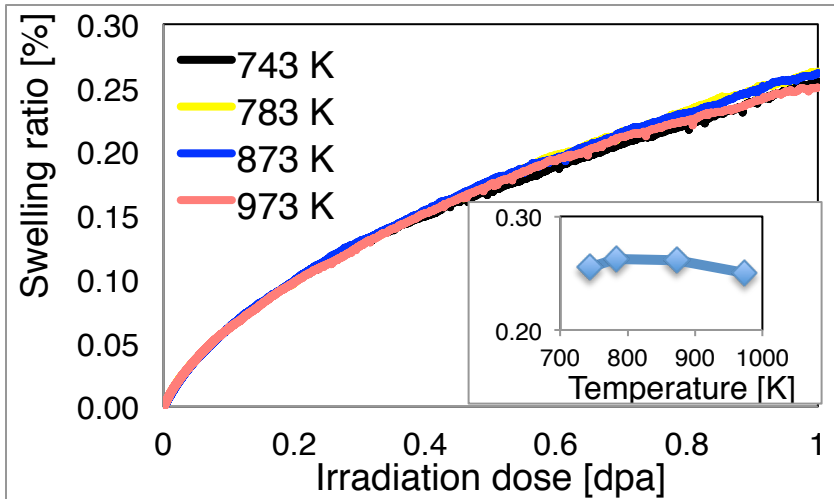


Figure 3: Evolution with dose of the swelling ratio as a function of temperature. The inset shows the amount of swelling after 1 dpa of irradiation.

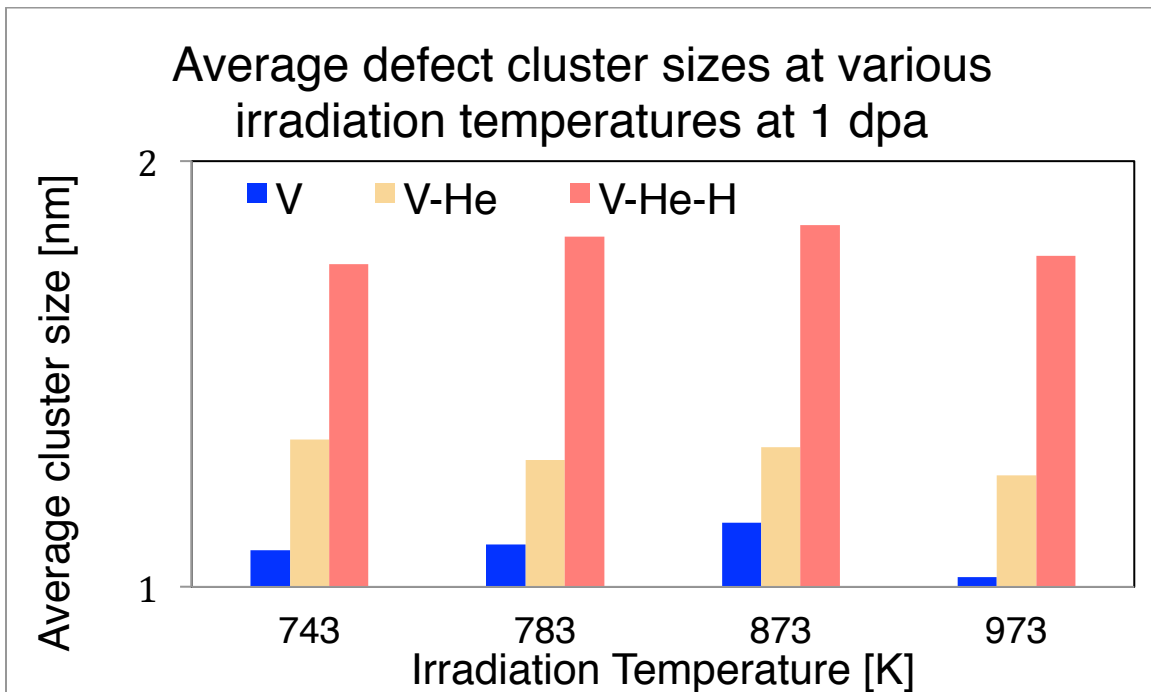


Figure 4: Average vacancy cluster size as a function of temperature after an accumulated dose of 1 dpa.

More striking perhaps is the average bubble size after 1 dpa, shown in Figure 4. There, it can be clearly seen that triple V-He-H clusters are significantly larger than their V-He and pure V counterparts. We note that at this dose level, the average size is still too small to be indicative of anything but bubble growth. In other words, 1 dpa is still well below the required dose to achieve runaway void growth and the bubbles are clearly in their growth phase.

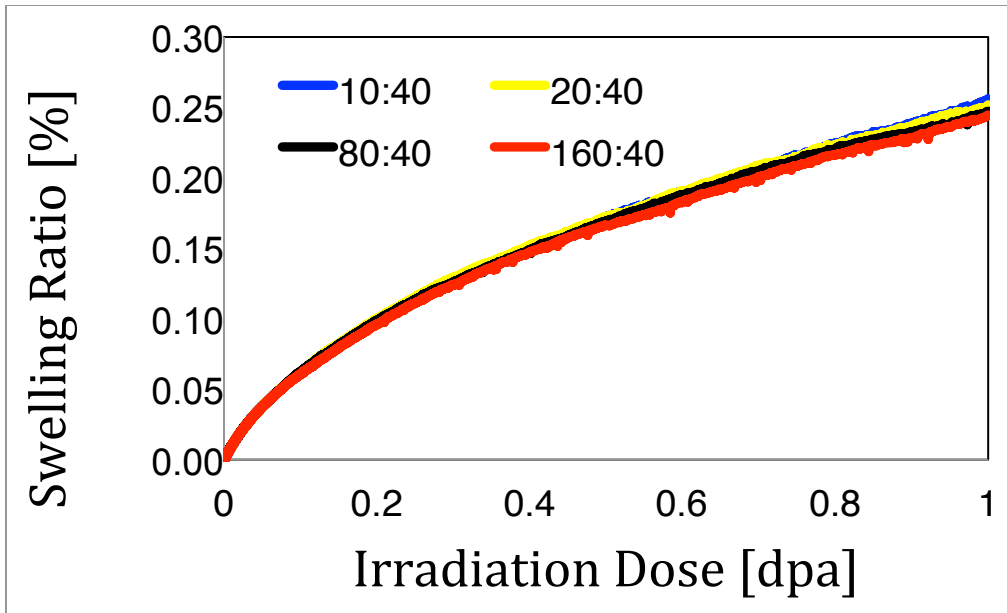


Figure 5: Effect on the swelling ration of the relative amount of He to H injected in the system.

We have also looked at the effect on swelling of the He-to-H insertion ratio. This is what is plotted in Figure 5 in terms of atomic parts per million per dpa for each species. Again, the differences are not remarkable, although clearly the higher the content of He relative to H, the lower the swelling. If one looks at the evolution with dose of the average bubble size with this ratio, shown in Figure 6, this trend is maintained, although it appears that there exists a threshold He-to-H level beyond which the bubble size does no longer change. This is the case for ratios of 80:40 and 160:40, where the average diameter saturates at about 1.2 nm, down from 1.8 nm at the fusion ratio of 10:40.

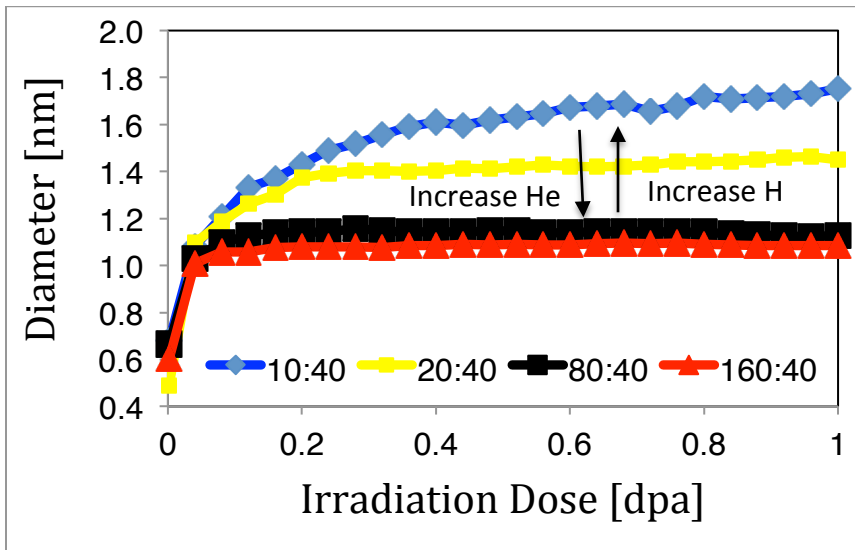


Figure 6: Evolution of the average bubble diameter with dose at 743 K as function of the He-to-H ratio.

Finally, we study the synergistic effect for the model of damage/He/H interaction described here. To this end, we plot in Figure 7 the average bubble size from three different simulations: (i) dual ion beam exposure with self-ions and H ions, (ii) dual ion beam exposure with self-ions and He, (iii) triple ion beam exposure with self-ions, He and H ions. Clearly, the triple beam case results in the largest bubbles (in the form of triple clusters).

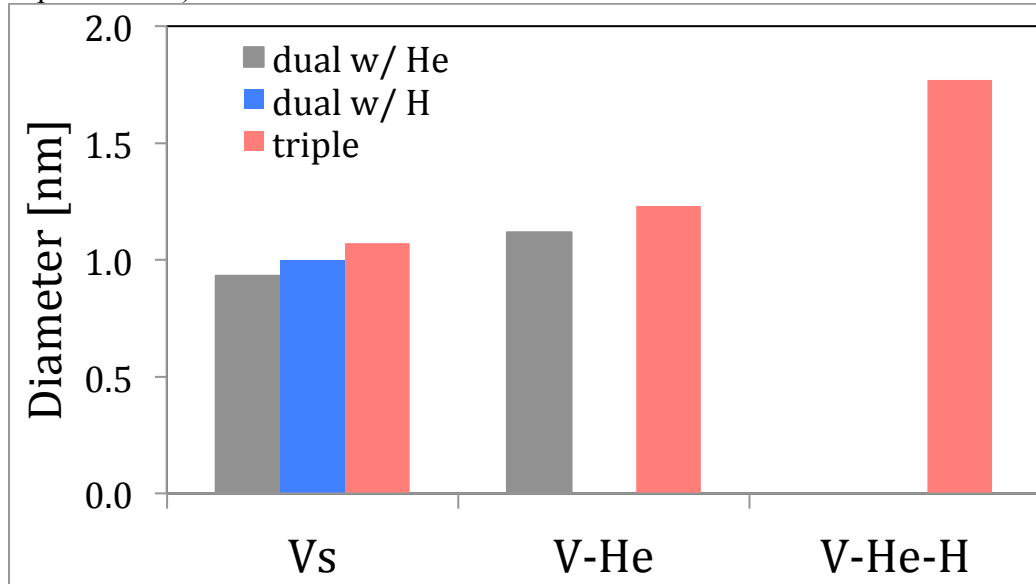


Figure 7: Average bubble diameter after 1 dpa of irradiation at 743 K under dual and triple ion-beam irradiation conditions.

6 Discussion and Summary

Our results do predict a significant influence of simultaneous He/H co-implantation on the average bubble size although not on the total amount of swelling. The available experimental evidence points to the importance of bubble/void size as the measure responsible for an increased swelling. Coexistence of He and H appears to limit the number density of available nucleation sites, resulting in much larger bubble sizes than when only He is present. This results in a lower cross section for SIA-bubble interaction, and hence an increased probability of SIA-loop trapping at sinks. In any case, the lack of difference in total swelling means that the current simulation model does not provide a mechanism for swelling increases in its present form. More work, both experimental and simulations, will have to be carried out to determine whether synergistic effects do indeed play an important role in the microstructural evolution of irradiated F/M steels.

This work performed under the auspices of the US Department of Energy by Lawrence Livermore National Laboratory under Contract DE AC52-07NA27344.

7 References

- [1] Haibo Liu, Mohamed A. Abdou, Larry R. Greenwood, *Fusion Engineering and Design* 88 (2013) 2860- 2864
- [2] G. R. Odette, T. Yamamoto, Y. Wu, E. Stergar, N. J. Cunningham, R. J. Kurtz, D. J. Edwards, *Fusion Reactor Materials Program* December 31, 2011 DOE/ER-0313/51 - Volume 51, p 90
- [3] R. Bullough, report: "Factors involved in the use of vanadium alloys and ferritic steels for the ITER first wall/blanket and divertor", UKAEA FUS 554, EURATOM/UKAEA Fusion, June 2009
- [4] Gilbert M.R. and Sublet J.-Ch. 2011 *Nucl. Fusion* 51 043005
- [5] M.R. Gilbert, S.L. Dudarev, S. Zheng, L.W. Packer and J.-Ch. Sublet, *Nucl. Fusion* 52 (2012) 083019 (12pp)
- [6] F.A. Garner, E.P. Simonen , B.M. Oliver , L.R. Greenwood , M.L. Grossbeck , W.G. Wolfer , P.M. Scott , *Journal of Nuclear Materials* 356 (2006) 122–135
- [7] F. Kano, Y. Arai, K. Fukuya, N. Sekimura and S. Ishino. *J. Nucl. Mater* 203 (1993) 151
- [8] K. Farrell and E. H. Lee, "Ion Damage in a Fe-10Cr-6Mo-0.5Nb Ferritic Steel," *Radiation-Induced Changes in Microstructure: I*, STP 955, American Society For Testing and Materials, Philadelphia, 1987, pp. 498-507.
- [9] F. A. Garner and L. R. Greenwood, *Radiation Effects and Defects in Solids*, 144 (1998) 251-283.
- [10] T. Ishizaki, Q. Xu, T. Yoshiie, S. Nagata, T. Troev, *J. Nucl. Mater.* 307–311 (2002) 961-965
- [11] G.D. Tolstolutsкая, V.V. Ruzhytskiy, I.E. Kopanets, S.A. Karpov, V.V. Bryk, V.N. Voyevodin, F.A. Garner, *J. Nucl. Mater.*, 356 (2006) 136-147
- [12] F.A. Garner, E.P. Simonen, B.M. Oliver, L.R. Greenwood, M.L. Grossbeck, W.G. Wolfer, P.M. Scott, *J. Nucl. Mater.*, 356 (2006) 122-135
- [13] F.A Garner, B.M Oliver, L.R Greenwood, M.R James, P.D Ferguson, S.A Maloy, W.F Sommer, *J. Nucl. Mater.*, 296 (2001) 66-82
- [14] S. Linderth, A. V. Shishkin, *Philos. Mag. A* 55 (3) (1987) 291
- [15] V. V. Kirsanov and M. V. Musina, *J. Nucl. Mater.* 191-194 (1992) 1318-1322
- [16] E. Hayward, C. Deo, *J. Phys.: Condens. Matter* 24 (2012) 265402
- [17] C. J. Ortiz, R. Vila, J. M. Pruneda, arXiv:1205.6374v2 [cond-mat.mtrl-sci]
- [18] Jaime Marian, Vasily V. Bulatov, *Journal of Nuclear Materials* 415 (2011) 84–95
- [19] T. Hoang, J. Marian, V. V. Bulatov, D. Chrzan, A. Arsenlis, P. Hosemann, submitted to *J. Comp. Phys* (2014)